# Reduction of Bearing Load Capacity and Increase in Volume Flow Due to Wall Slip

**Maximilian M. G. Kuhr, M.Sc., Tobias Corneli, M.Sc., Univ.-Prof. Dr.-Ing. Peter F. Pelz, Institut für Fluidsystemtechnik (FST), Technische Universität Darmstadt, Germany**

## 1 Introduction

Since the beginning of the 20th century, hydraulic sealings and journal bearings are designed employing Reynolds lubrication theory /1–3/. The Reynolds lubrication theory presumes the no slip boundary condition at the liquid-solid interface. Recent studies conducted by the authors show, that the assumed no slip boundary condition at the liquid-solid interface is not valid for most fluid power applications; cf. /4/. This effects the prediction of leakage flow and frictional behaviour of sealing systems as well as bearing capacity of journal bearings. Thus, considering slip at the liquid-solid interface is important for the design of hydraulic components. The concept of wall slip was already discussed by Navier /5/ and Stokes /6/, when deriving the momentum equation for Newtonian fluids in the 19th century. Stokes favours the no slip boundary condition and justifies his hypothesis by a good agreement of the theory with experimental investigations of Poiseuille /7/. In contrast, Navier /5/ formulates the slip boundary condition, with the slip velocity being the product of the shear rate and the slip length. Regardless of this discussion, the no slip boundary condition is established over the centuries, based on the insufficient measurement techniques. However, in many technically important applications of fluid power technologies wall slip is not negligible. This is the case if the quotient of slip length and typical flow geometry is less than 10E-3. Thus, for typical hydraulic systems is reasonable to consider slip, if the gap geometries are of the order of magnitude of 10 µm.

## 2 Navier slip boundary condition and generalised Reynolds Equation

Interesting is the train of thought, which Navier causes to formulate the slip boundary condition in 1822 /5/: Navier interprets the processes at the wall as a dynamic equilibrium between the shear force of the liquid at the wall $\mu\,\partial u/\partial n$ and the wall-parallel adhesive forces (dynamic viscosity $\mu$). The adhesive forces are proportional to the slip velocity $u_s$, conforming to Stoke's law. Hence the balancing yields

$$u_s * k = \mu \frac{\partial u}{\partial n}. \tag{1}$$

Today $k$ is called the friction coefficient. Helmholtz /8/ interprets the constant in Navier's relationship by means of dimensional analysis as a length, the nowadays called slip length $\lambda$

$$\lambda := \frac{\mu}{\text{const}}. \tag{2}$$

Thus, (1) yields the purely kinematic form

$$u_s = \lambda \frac{\partial u}{\partial n}. \tag{3}$$

known today, no longer revealing Naviers original thought and dynamic nature of the boundary condition.

Sometimes an anisotropic dynamic viscosity is introduced as a phenomenological model. I.e. the viscosity near the wall is considered to be smaller than in the bulk. This concept has to be judged critical from a scientific point of view. For a wall viscosity boundary layer the viscosity and boundary layer thickness has to be given, whereas for Naviers boundary condition only the slip length $\lambda$ or alternatively the friction coefficient has to be quantified. The concept of anisotropic viscosity is therefore no scientific progress, rather a drawback.

*Figure 1* illustrates the geometrical interpretation of the slip length

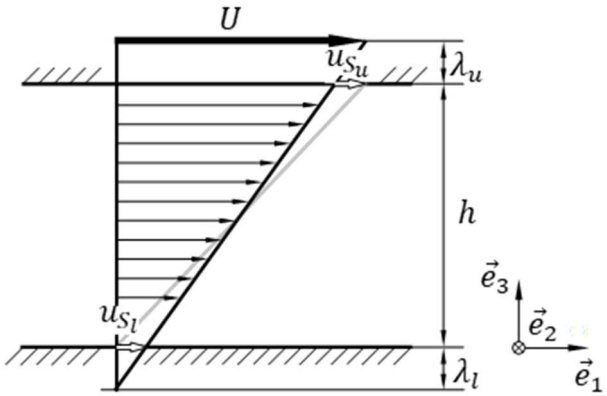


*Figure 1: Simple shearing flow for no slip (grey) and slip (black)*

by means of a simple shearing flow example. It shows the velocity profiles for no slip boundary condition (grey) and Navier slip boundary condition (black). The lower surface is fixed while the upper surface moves with constant velocity $U$ at a distance $h$. *Figure 1* also illustrates the geometrical interpretation of the slip length by means of a simple shearing flow example. It shows the velocity profiles for no slip boundary condition (grey) and Navier slip boundary condition (black). In the case of no-slip, the velocity of the liquid molecules at the wall is identical to the wall velocity. In the case of slip, there is a relative velocity between the wall near molecules of the liquid and the wall. The relative velocity at the fixed wall $u_{s_1}$ is greater than zero and the relative velocity at the moving wall $u_{s_2}$ reduces the liquid velocity relative to the wall velocity $U$. Extrapolating the velocity profile down to zero and up to the surface velocity $U$ yields the slip length as the perpendicular distance from the surface to the boundaries of the extrapolated velocity profile. Due to this, Helmholtz's [8] geometric

interpretation of an apparent gap opening due to wall slip is deduced. Slip velocity and shear rate are proportional and the proportionality constant is the slip length.

So far, the Reynolds equation is derived and applied only assuming no-slip boundary condition. Since wall slip affects both the leakage flow of seals and the bearing capacity of plain bearings, it is necessary to solve the Reynolds equation while taking the dynamic slip boundary condition into account. The generalized Reynolds equation incorporating wall slip can be derived in five steps.

Starting from the well-known assumptions of the Reynolds equation (cf. /9/), i.e. $\alpha Re \ll 1$, the Navier Stokes equation simplify to the linear differential equations

$$\frac{\partial p}{\partial x_1} = \mu \frac{\partial^2 u_1}{\partial x_3^2}; \quad \frac{\partial p}{\partial x_2} = \mu \frac{\partial^2 u_2}{\partial x_3^2}; \quad \frac{\partial p}{\partial x_3} = 0. \tag{4}$$

By integrating the linear differential equation twice, the general solution of the velocity distribution in the lubrication gap is derived. Applying Navier's slip boundary condition for the velocities $u$ at the fixed $(x_3 = 0)$ and the moving wall $(x_3 = h)$

$$u_i(x_3 = 0) = \lambda_l \left.\frac{\partial u_i}{\partial x_3}\right|_{x_3=0}, \tag{5}$$

$$u_i(x_3 = h) = U_i - \lambda_u \left.\frac{\partial u_i}{\partial x_3}\right|_{x_3=h(x_i)}, \tag{6}$$

yields the special solution of the velocity distribution for $i = 1, 2$. Substituting the integration constants using the boundary conditions from Equation (5) and (6) provides the solution to the boundary value problem, with $h = h(x_i, t)$. The volume flow $q$ per unit depth in the $x_i$-direction, is obtained by integrating the velocity distribution across the lubrication gap height.

$$q_i(t) = \frac{U_i h}{2} \frac{1 + 2\lambda_l/h}{1 + \lambda_l/h + \lambda_u/h} - \frac{h^3}{12\mu} \frac{\partial p}{\partial x_i} \frac{1 + 4\lambda_l/h + 4\lambda_u/h + 12\lambda_l\lambda_u/h^2}{1 + \lambda_l/h + \lambda_u/h}. \tag{7}$$

Inserting (7) into the integral form of the continuity equation yields the generalized Reynolds equation for plane flows. New is the now included wall slip.

$$\frac{\partial}{\partial x_i}\left[\frac{h^3}{\mu}\frac{\mathrm{d}p}{\mathrm{d}x_i}\left(\frac{1 + 4\lambda_l/h + 4\lambda_u/h + 12\lambda_l\lambda_u/h^2}{1 + \lambda_l/h + \lambda_u/h}\right)\right] = \tag{8}$$

$$= \frac{\partial}{\partial x_i}\left[6U_i h\left(\frac{1 + 2\lambda_l/h}{1 + \lambda_l/h + \lambda_u/h}\right)\right] + \frac{\partial h}{\partial t}.$$

### *2.1 Application to Slider Bearings*

The pressure distribution in the plane lubrication gap of a slider bearing as well as the increased volume flow is investigated, taking Navier's slip boundary condition into account; cf. *Figure 2*. The upper wall is inclined by the angle $\alpha$ with respect to the $x$ - axis and moves at the constant velocity $U$. The liquid is pulled into the narrowing gap, leading to a pressure increase. So far, the load-bearing capacity for this arrangement is only examined for the no-slip boundary condition. In the following, the influence of wall slip is considered as well.

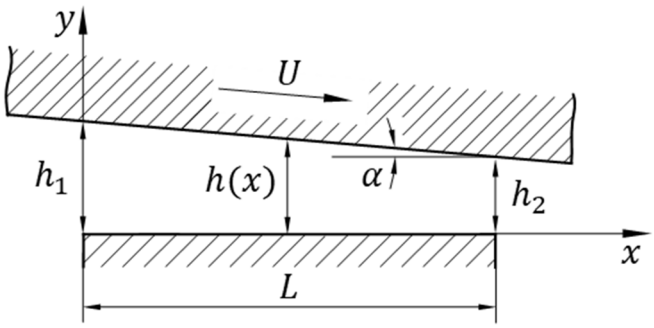


*Figure 2: Slider bearing*

Deriving the bearing capacity of the slider bearing, it is assumed for simplicity that both the fixed and moving wall are of the same material and Temperature, thus the slip length is identical at both solid-liquid interfaces: $\lambda_l = \lambda_u = \lambda$. Under this assumption and for quasi-stationary flow, the modified Reynolds equation (8) reads

$$\frac{\mathrm{d}}{\mathrm{d}x}\left[\frac{h^3}{\mu}\frac{\mathrm{d}p}{\mathrm{d}x}\left(\frac{1+8\lambda^2/h+12\lambda^2/h^2}{1+2\lambda/h}\right)\right] = \frac{\mathrm{d}}{\mathrm{d}x}(6Uh). \tag{9}$$

Integration of (9) leads to

$$\frac{h^3}{\mu}\frac{\mathrm{d}p}{\mathrm{d}x}\left(\frac{1+8\lambda^2/h+12\lambda^2/h^2}{1+2\lambda/h}\right) = 6Uh + C_1\,. \tag{10}$$

The integration constant $C_1$ is determined at the location $x = \bar{x}$ of maximum pressure, where $\mathrm{d}p/\mathrm{d}x = 0$, giving the pressure gradient depending on the gap height $h(x)$ and the gap height at maximum pressure $\bar{h}$

$$\frac{\mathrm{d}p}{\mathrm{d}x} = 6\mu U\frac{1-\bar{h}/h}{h(6\lambda+h)}\,. \tag{11}$$

With the gap height $h(x) = h_1 - \alpha x$ and substituting $\mathrm{d}x = -\mathrm{d}h/\alpha$, the pressure distribution yields

$$p(h(x)) = -\frac{6\mu U}{\alpha}\int \frac{1-\overline{h}/h}{h(6\lambda+h)}\mathrm{d}h \tag{12}$$

Applying the boundary condition $p(x=0) = p(h_1) = 0$ the integration constant can be determined. Determining the position of the maximum pressure $\bar{h}$ at $p(x=L) = p(h_2) = 0$ resulting in the pressure distribution and the position of the maximum pressure.

$$p(h) = \frac{\mu U}{6\alpha\lambda^2}\left[\left(\bar{h}+6\lambda\right)\left[\ln\left(\frac{h+6\lambda}{h_1+6\lambda}\right)-\ln\left(\frac{h}{h_1}\right)\right]+6\bar{h}\lambda\left(\frac{h-h_1}{hh_1}\right)\right], \tag{13}$$

$$\overline{h} = \frac{6\lambda\left[\ln\left(\frac{h_2+6\lambda}{h_1+6\lambda}\right)+\ln\left(\frac{h_1}{h_2}\right)\right]}{\ln\left(\frac{h_1+6\lambda}{h_2+6\lambda}\right)+\ln\left(\frac{h_2}{h_1}\right)+6\lambda\left(\frac{h_1-h_2}{h_2h_1}\right)}. \tag{14}$$

With the made assumptions, inserting (13) into (7) leads to the volume flow per unit depth of the slider bearing including slip

$$q = \frac{3U\lambda\left[\ln\left(\frac{h_2}{h_1}\right)+\ln\left(\frac{h_1+6\lambda}{h_2+6\lambda}\right)\right]}{6\lambda\left(\frac{h_2-h_1}{h_2h_1}\right)+\ln\left(\frac{h_1}{h_2}\right)+\ln\left(\frac{h_2+6\lambda}{h_1+6\lambda}\right)}. \tag{12}$$

## 3 Darmstadt Slip Length Tribometer

The Darmstadt Slip length Tribometer (DSLT) /4, 10/ is an indirect measuring method for quantifying wall slip. The slip length is determined by the measurement of an integral quantity and a suitable model. The integral measured quantity is hereby the friction torque between rotating and the stationary disk depending on the gap height. As a suitable model, the Reynolds equation (8) is used.

The DSLT is a classical plate-plate tribometer (cf. *Figure 3*) measuring the friction torque transmitted from the rotating disk through the liquid film of height h to the stationary disk. The torque is measured with a reaction torque sensor at the stationary disk. The distance is measured by means of integrated capacitive distance sensors with a resolution of 4 nm. In order to allow a cardanic self-levelling of the two disks relative to each other, the lower one is supported by a jewel bearing. The adjustment of the lubrication gap is achieved by the axial spring stiffness and the feed pressure of the test liquid.

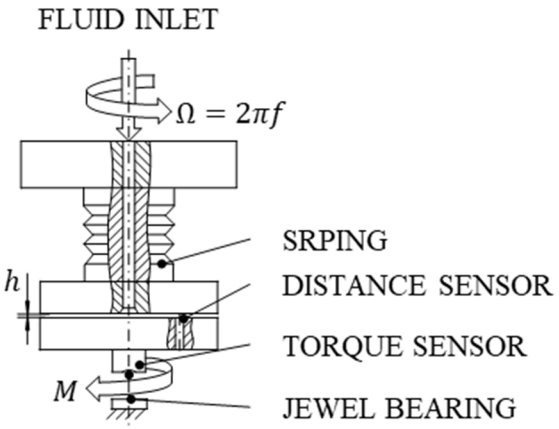


*Figure 3: Principle sketch of the slip length tribometer with a disk diameter of 64 mm*

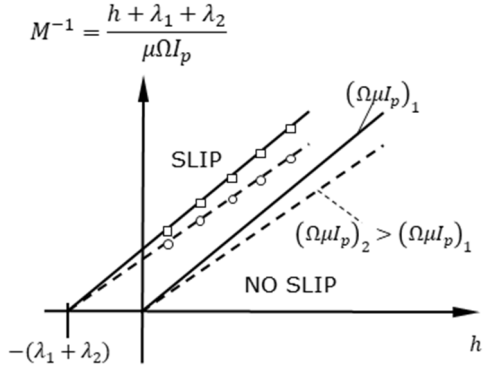


*Figure 4: Inverse friction torque depending on the gap height for slip and no slip boundary condition*

In the lubrication gap, the pressure flow in radial direction and the drag flow in circumferential direction are superimposed. For small gap heights, the Reynolds number is of the order of magnitude of 0.1 and the tilt angle of the disks is smaller than 0.001°. Thus the Reynolds equation (8) for wall slip can be used, giving the Couette velocity profile $u(r, y) = \Omega r(y + h)/(h + \lambda_1 + \lambda_2)$. With the velocity profile in the circumferential direction, the friction torque is determined by integrating the shear stresses.

$$M^{-1} = \frac{h + \lambda_1 + \lambda_2}{\mu \Omega I_p}. \tag{13}$$

The inverse of the friction torque is a linear equation with the polar moment of area $I_P = \int_A r^2 \mathrm{d}A$, the sum of the slip lengths at the stationary and rotating disk can be obtained by determining the $x$-axis intercept for the curve of the equation.

*Figure 4* illustrates schematically the relationship of equation (13) for Newtonian fluids. The inverse friction torque depends linearly on the gap height. As the no-slip boundary condition holds true, the linear curve of the inverse friction torque intersects the coordinate origin. As the rotational frequency of the rotating disks increases, the slope of the straight-line equation decreases. If wall slip occurs at the liquid-solid interface, the curve intersects the $x$-axis in the negative. This distance is equal to the sum of the two slip lengths at the stationary and the rotating disk.

## 4 Results

### *4.1 Slip length measurement*

*Figure 5* shows the measurement of the inverse torque as a function of varying gap heights, showing the $M^{-1}$- $h$ - curve for an alpha-olefin 6 at constant temperature of $29.9°\mathrm{C}$ and constant rotational frequency of $2\ \mathrm{Hz}$. The symbols mark the individual measurement points at which the torque was measured depending on the gap height. The figure shows 20 measurement series. The best fit linear regression curve is determined individually for each measurement series and the slip length is determined from the intersection with the $x$-axis.

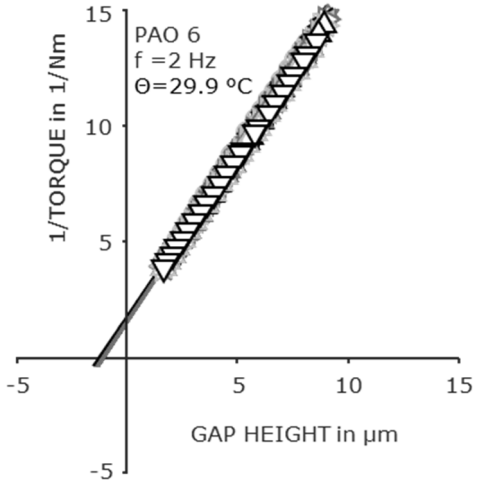


*Figure 5: Slip length measurements for POA 6*

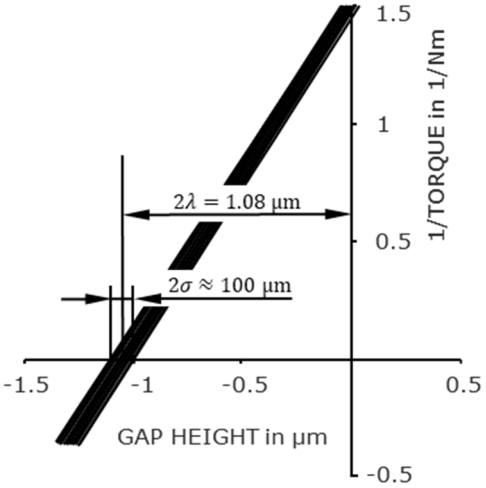


*Figure 6: Detailed view of the intersection*

*Figure 6* gives a detailed view at the intersection of the regression curves with the $x$-axis. The measured slip length for an alpha-olefin at $29.9°\mathrm{C}$ averages to $\lambda = 540\ \mathrm{nm}$. The measurements can be repeated with a standard deviation of $\sigma = 50\ \mathrm{nm}$. Due to the 20 repetitions, the statistical uncertainty is reduced by the factor $t/\sqrt{n}$ (student-

t-distribution). The statistical uncertainty of the measured value with $n = 20$ repetitions and a confidence interval of 95% is less than 24 nm and thus less than 5% of the measured mean value.

### *4.2 Bearing capacity and volume flow of a slider bearing*

*Figure 7* gives the pressure distribution in a lubrication gap for the slip as well as for the no slip boundary condition applying Equation (13).

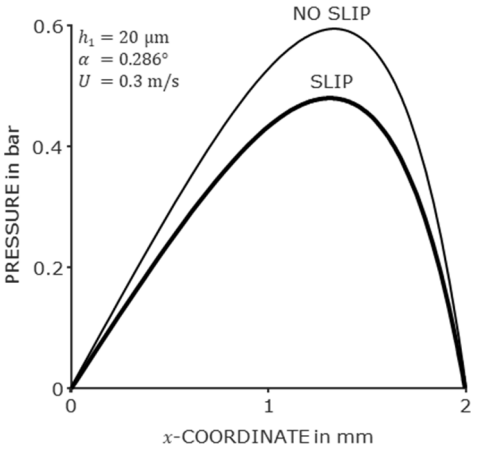


*Figure 7: Pressure distribution in the lubricated gap*

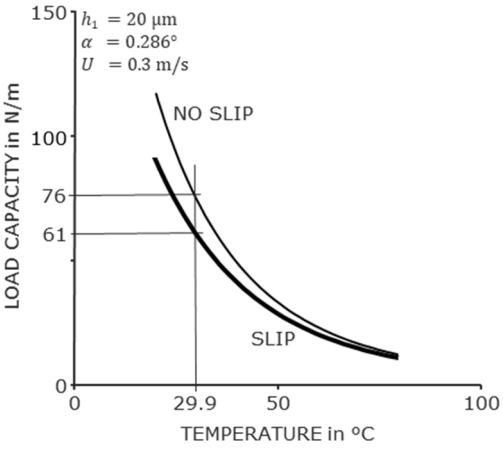


*Figure 8: Load capacity of the slider bearing*

The gap height $h_1$ is $20\ \mu m$, the tilt angle $\alpha$ of the upper plate is 0.286° and the plate is moved at constant velocity $U$ of 0.3 m/s. The utilized fluid is an alpha-olefin with a dynamic viscosity $\mu$ of 0.039 Pa·s and a slip length $\lambda$ of 540 nm at 29.9 °C. The quotient of slip length and typical flow geometry $h_1$ is thus 0.027. *Figure 7* exhibits, that the peak pressure is reduced due to slip by approximately 20 %. Integrating the pressure along the horizontal directions yields the load capacity per unit depth, which is also reduced by approximately 20 %.

Hydraulic applications operate in a wide temperature range. Thus the thermal behaviour of the load capacity and leakage flow is of major interest. The temperature dependent dynamic viscosity and the temperature dependent slip length are obtained by means of Arrhenius relations; cf. /4/. Using these Arrhenius relations, *Figure 8* gives the temperature depending load capacity of the above mentioned slider bearing. The presented results clearly show that difference in load capacity per unit depth for slip and no slip decreases with increasing temperature. This is reasonable since the activation energy for wall slip is smaller than the activation energy for shearing, cf. /4/.

*Figure 9* gives the temperature depending volume flow per unit depth of the slider bearing using equation (12) and the Arrhenius relation for the temperature dependence of the slip length. At 29.9 °C the volume flow including slip increases in contrast

to the no-slip solution by approximately 0.75 %. With increasing system temperature, the volume flow including slip starts to approach the no-slip values.

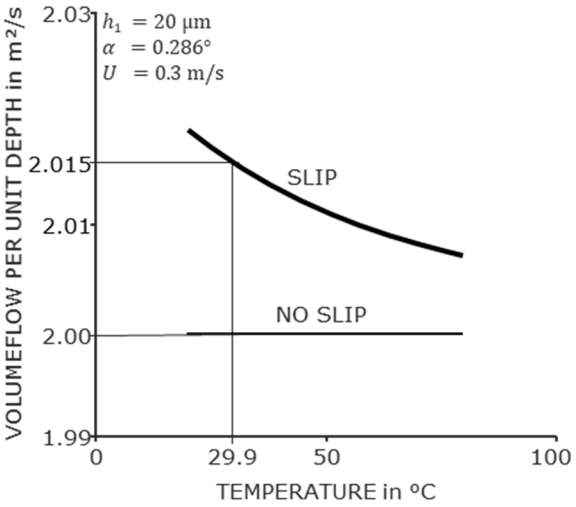


*Figure 9: Volume flow $q_x$ per unit depth*

## 5 Summary and Conclusion

The presented paper investigates the temperature dependence of the Navier slip boundary condition and the related reduction of load capacity of a bearing and the increased volume flow. First, the Navier slip boundary condition is discussed and a modified Reynolds equation, including slip, is derived. Second, the modified Reynolds equation, the pressure distribution and the load capacity of a slider bearing as well as the corresponding volume flow are deduced. Third, the Darmstadt Slip Length Tribometer is presented, utilized for measuring the slip length of technical rough surfaces. Finally, the paper closes with the comparison of the temperature dependent results of the slip length measurements and the effect on the load capacity of the slider bearing as well as the increased volume flow in comparison to the common no slip boundary condition. In future further efforts have to be made in understanding the effects on the temperature-dependent sliding length. In a first step the molecular structure of the oil has to be varied. Afterwards the influence of surface roughness on the slip length needs further investigation. In a final step, the influence of different material combinations should be addressed.

## 6 Acknowledgements

The authors thank the Research Association for Fluid Power of the German Engineering Federation VDMA for its financial support. Special gratitude is expressed to the participating companies and their representatives in the accompanying industrial committee for their advisory and technical support.

## 7 Nomenclature

| *Variable* | *Description* | *Unit* |
|---|---|---|
| $f$ | frequency | $T^{-1}$ |
| $h$ | height | $L$ |
| $\overline{h}$ | height at maximum pressure | $L$ |
| $M$ | torque | $L^2 M T^{-2}$ |
| $p$ | pressure | $L^{-1} M T^{-2}$ |
| $q$ | volume flow | $L^3 T^{-1}$ |
| $U$ | velocity of the slider bearing | $L T^{-1}$ |
| $u$ | velocity | $L T^{-1}$ |
| $\alpha$ | angle | $*$ |
| $\Theta$ | temperature | $\Theta$ |
| $\lambda$ | slip length | $L$ |
| $\mu$ | dynamic viscosity | $L^{-1} M T^{-1}$ |
| $\Omega$ | angular velocity | $T^{-1}$ |

## 8 References

/1/ Müller, H.K.: Abdichtung bewegter Maschinenteile. Funktion - Gestaltung - Berechnung - Anwendung. Müller, Waiblingen (1990)

/2. Petrov, N.P., Reynolds, O., Sommerfeld, A., Michell, A.G.M., Hopf, L. (eds.): Abhandlungen über die hydrodynamische Theorie der Schmiermittelreibung. Ostwald's Klassiker der exakten Wissenschaften, vol. 218. Akad. Verl.-Ges, Leipzig (1927)

/3/ Trutnovsky, K.: Die Dichtung bewegter Maschinenteile. In: Berührungsdichtungen

/4/ Corneli, T., Pelz, P.F.: The Activation Energy for Wall Slip. submitted to Phyiscal Review Letters, 2017

/5/ Navier, M.: Mémoires de l'Académie des Sciences de l'Institut Impérial de France. Firmin Didot (1827)

/6/ Stokes, G.G. (ed.): Mathematical and Physical Papers. Cambridge Library Collection - Mathematics. Cambridge University Press, Cambridge (2009)

/7/ Poiseuille, J.L.: Recherches experimentales sur le mouvement des liquides dans les tubes de tres-petits diametres. Imprimerie Royale (1844)

/8/ Helmholtz, H.: Über Reibung tropfbarer Flüssigkeiten. Von H. Helmholtz und G. v. Piotrowski. (Mit 2 Taff.) (Aus d. XL. Bd. S. 607. 1860. der Sitzgsber. der math-nat. Cl. der k. Ak. der Wiss. bes. dbg.). Hof- & Stts.-Druck (1860)

/9/ Spurk, J.H., Aksel, N.: Strömungslehre. Einführung in die Theorie der Strömungen, 8th edn. Springer-Lehrbuch. Springer-Verlag Berlin Heidelberg, Berlin, Heidelberg (2010)

/10/ Corneli, T., Pelz, P.F., Ludwig, G.: Slip length in narrow sealing gaps an experimental approach. In: 18th International Sealing Conference, Stuttgart (2014)